Miscible Blends of Two Crystalline Polymers. 1. Phase Behavior and Miscibility in Blends of Poly(vinylidene fluoride) and Poly(1,4-butylene adipate)

J. P. Penning[†] and R. St. John Manley*

Department of Chemistry, McGill University, 3420 University Street, Montréal, Québec H3A 2A7, Canada

Received May 15, 1995; Revised Manuscript Received September 30, 1995[⊗]

ABSTRACT: The phase behavior and miscibility of blends of poly(vinylidene fluoride) (PVF_2) and poly(1,4-butylene adipate) (PBA), both semicrystalline polymers, have been investigated using differential scanning calorimetry and light-scattering techniques. The phase diagram of this blend system exhibits a single glass transition temperature over the entire composition range, two distinct melting transitions, and a cloud-point curve above a lower critical solution temperature of 235 °C. A depression of the equilibrium melting point of both PVF_2 and PBA is observed. From the melting point data of the high-T_m component, PVF_2, a value for the polymer−polymer interaction parameter of $\chi_{12} = -0.19$ was derived using the Flory−Huggins equation. This implies that PVF_2/PBA blends are thermodynamically miscible in the melt. The extent of the melting point depression for the low-T_m component, PBA, is much smaller than it is for PVF_2, which is attributed to the fact that PVF_2 is semicrystalline at temperatures of PBA melting. Infrared spectroscopy measurements focusing on the carbonyl absorption band of PBA reveal a slight shift in peak position toward lower frequencies due to blending, indicating that the thermodynamic miscibility of the PVF_2/PBA pair arises from weak specific interactions involving the polyester carbonyl group. In spite of their miscibility, blends of PVF_2 and PBA exhibit a complex phase behavior and may form multiphase systems. Of particular interest is the three-phase morphology in which two distinct crystalline phases (PBA and PVF_2) coexist with an intimately mixed amorphous phase. This morphology is observed at room temperature over a very broad composition range.

Introduction

In the past two decades, a considerable amount of research has been aimed at gaining a better understanding of the miscibility of polymers and, to this end, a great number of miscible polymer pairs has been studied.[1,2] Most of the systems investigated represent mixtures of two amorphous polymers, such as poly(styrene)/poly(phenylene oxide), or mixtures in which one of the components is semicrystalline, such as poly(vinyl chloride)/poly(caprolactone). On the other hand, blends in which *both* components are semicrystalline polymers have received much less attention than fully amorphous or amorphous/semicrystalline systems. Semicrystalline/semicrystalline polymer blends, however, may be of considerable technological interest, and the study of these systems may provide new insights into the miscibility, crystallization behavior and morphology of polymer blends in general. Semicrystalline/semicrystalline polymer blends that have been reported in the literature include poly(vinylidene fluoride) with stereoregular poly(acrylates),[3,4] poly(ethylene oxide)/poly(hydroxybutyrate),[5] poly(vinylidene fluoride)/poly(3-hydroxybutyrate),[6] poly(caprolactone)/poly(carbonate),[7−10] and blends of linear and branched polyethylenes.[11] Only for the last two systems has the overall phase behavior and morphology been examined in considerable detail.[7−11]

The aim of the present study is to gain a better understanding of semicrystalline/semicrystalline polymer mixtures and to establish to what extent the current knowledge of polymer blends applies to these complex systems. In this study, we have chosen the mixture of poly(vinylidene fluoride) (PVF_2) and poly(1,4-butylene adipate) (PBA) as a model system. These polymers are both crystallizable and, in the pure state, readily undergo crystallization over a range of temperatures. Their melting points (ca. 60 °C for PBA and ca. 160 °C for PVF_2) lie within an accessible temperature range and are some 100 deg apart, so the melting behavior and crystallization occurring in both PVF_2 and PBA phases can be studied separately. The crystallization behavior of PVF_2 has been widely studied, in the bulk[12−19] as well as in blends,[4,20−22] because of the crystalline polymorphism of PVF_2 and the unique piezoelectric properties[23] exhibited by certain crystal modifications of this polymer. It has been shown[24] that PVF_2 is miscible with a number of carbonyl-containing polymers, and it is therefore quite possible that PVF_2 will form miscible blends with PBA.

In this study, the phase behavior and miscibility of the PVF_2/PBA system is investigated in terms of its phase diagram, which has been established using differential scanning calorimetry (DSC) and cloud-point measurements. It turns out that PVF_2/PBA blends exhibit a single, composition dependent glass transition temperature and that the equilibrium melting point of the PVF_2 component is depressed upon mixing with PBA. Above the melting point of the higher melting component, PVF_2, the blends form optically clear melts which undergo liquid−liquid phase separation above a lower critical solution temperature (LCST) of 235 °C. These results quite convincingly demonstrate the miscible nature of this polymer pair. FT-IR studies indicate that the miscibility arises from specific interactions involving the carbonyl group in PBA, since the C=O stretching frequency of PBA in the mixed state is shifted slightly as compared to pure PBA.

Although PVF_2 and PBA are miscible in the melt, their mixtures exhibit a complicated phase behavior, leading to the formation of highly interesting morphol-

* To whom correspondence should be addressed.
[†] Present address: Akzo-Nobel Central Research, Department RDS, P.O. Box 6300, 6800 SB Arnhem, The Netherlands.
[⊗] Abstract published in *Advance ACS Abstracts,* November 15, 1995.

0024-9297/96/2229-0077$12.00/0

ogies and supermolecular structures consisting of up to three separate phases. In this sense, PVF_2/PBA mixtures provide a unique opportunity for studying the relations between phase behavior and structure formation in miscible polymer blends. Investigations of the blend morphology and of the kinetics of the various phase transitions (including liquid−liquid phase separation and crystallization) are currently underway and will be described in separate papers.

Experimental Section

Materials. The PVF_2 sample used in this study (M_w = 140 000) was supplied by Polysciences Inc. (Warrington, PA) and was used as received. The PBA sample was obtained from Scientific Polymer Products, Inc. (Ontario, NY) and was purified by reprecipitation from *N*,*N*-dimethylformamide (DMF) into cold methanol (−10 °C). The as-precipitated PBA has M_n = 9800 and M_w = 14 050, as determined by gel permeation chromatography using 1,4-dioxane as eluent.

Blends of PVF_2 and PBA were prepared by solvent casting using DMF as a mutual solvent. Stock solutions of both polymers (initial concentration 2 g/100 mL) were mixed in the desired proportions, well stirred, and subsequently cast onto Teflon dishes. The solvent was allowed to evaporate in a controlled airstream for 24 h, and the resulting films were further dried in vacuum at room temperature for 3 days. In this way, blends were prepared in various compositions ranging from 90/10 to 10/90 in ratio of weight percent, the first numeral referring to PVF_2 throughout this paper.

Measurements. Thermal transitions of the blends were measured by means of differential scanning calorimetry (DSC) using a Perkin-Elmer DSC-7 equipped with an Intracooler system. The temperature readings of the instrument were calibrated using high-purity octadecane and indium standards. Sealed aluminum sample pans containing 2−5 mg of blend material were used in all experiments. At the beginning of each experiment, the sample was heated at 200 °C for 10 min so as to destroy its initial crystallinity. Melting transitions were recorded at a scanning rate of 5 °C/min, and the melting point was obtained from the peak temperature of the endotherm. The degree of crystallinity of both PVF_2 and PBA components was calculated from the area under their respective melting endotherms, using the value of the heat of fusion of 100% crystalline material (93.2 J/g for PVF_2[15] and 107.3 J/g for PBA[25]) and normalizing with respect to blend composition. For the determination of glass transition temperatures, the instrument was cooled using liquid nitrogen and operated at a scanning rate of 20 °C/min.

Fourier transform infrared (FT-IR) spectroscopy on various blends was performed using a Perkin-Elmer FT-IR microscope equipped with a mercury cadmium telluride detection system, connected to a Perkin-Elmer Model 16PC spectrophotometer. Transmission spectra in the region from 4000 to 400 cm^{-1} were obtained by signal-averaging 200 scans at 2 cm^{-1} resolution. The microscope was equipped with a Mettler FP52 hot-stage which allowed spectral measurement at elevated temperatures. This setup required the use of special NaCl transmission windows, which were obtained from Wilmad Glass Co., Inc. (Buena, NJ).

The cloud-point temperatures of various blends were measured at the Institute of Polymer Engineering, University of Akron, using a light-scattering technique, as is described in more detail elsewhere.[26]

Results and Discussion

Phase Behavior. The overall phase diagram of the PVF_2/PBA blend system, as it was established using thermal analysis and light-scattering techniques, is depicted in Figure 1. The data shown represent the actual (thermodynamic) phase equilibria, with the exception of the glass transition temperatures which were determined at a heating rate of 20 °C/min. It is evident from Figure 1 that the pure components undergo only two phase transitions, a glass transition (T_g) and melting (T_m), whereas their mixtures, in the central range of compositions, exhibit four phase transitions: a single glass transition, two melting transitions and demixing above a lower critical solution temperature (LCST). The phase diagram indicates that PVF_2 and PBA are compatible in the melt and, at the same time, that their mixtures will form a one-phase, homogeneous system only within a specific composition−temperature window. This one-phase region is located between the PVF_2 liquidus and the cloud-point curve. Raising the temperature from the one-phase region will eventually lead to liquid−liquid phase separation. Lowering the temperature to $T < T_m(PVF_2)$ will cause the PVF_2 component to crystallize and thus to segregate from the mixture. In this temperature regime, the blends are amorphous/semicrystalline. Further lowering of the temperature to $T < T_m(PBA)$ will induce crystallization of the PBA component, leading to a three-phase morphology in which two distinct crystalline phases coexist with a mixed amorphous phase. These materials may be classified as semicrystalline/semicrystalline blends. The process of crystallization of the two blend components leading to the semicrystalline/semicrystalline state is illustrated in Figure 2, which shows the DSC traces for a 50/50 blend recorded during cooling from 200 °C to subambient temperatures. The traces exhibit two distinct exothermic peaks resulting from the crystallization of PVF_2 and PBA. This behavior is observed at moderate (20 °C/min) as well as high (200 °C/min) cooling rates. Thus, PVF_2/PBA blends will exhibit two distinct crystalline phases at room temperature under almost any experimental condition. In addition, the crystallization of PVF_2 is complete before crystallization of PBA commences, showing that the two polymers

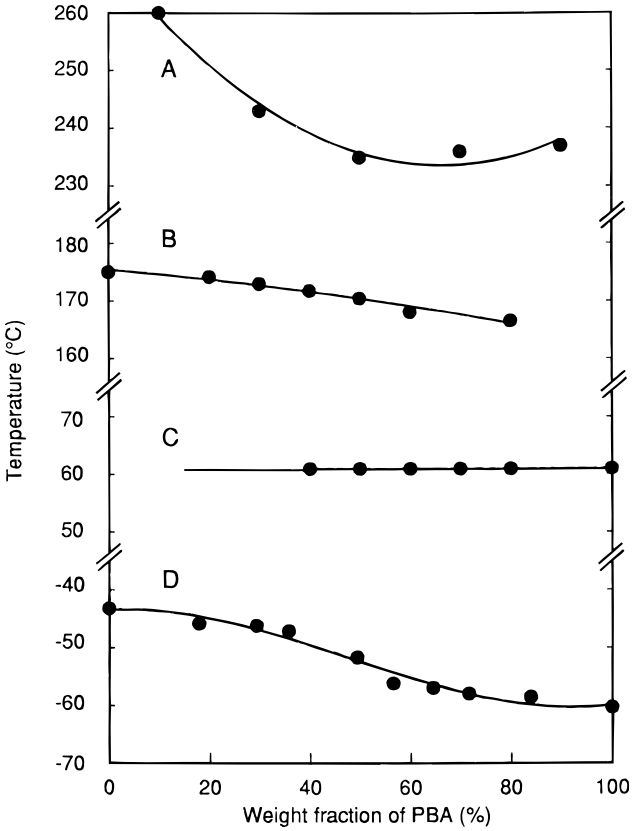

Figure 1. Phase diagram of PVF_2/PBA blends showing the cloud-point curve (A), the equilibrium melting temperatures of PVF_2 (B) and PBA (C), and the glass transition (D).

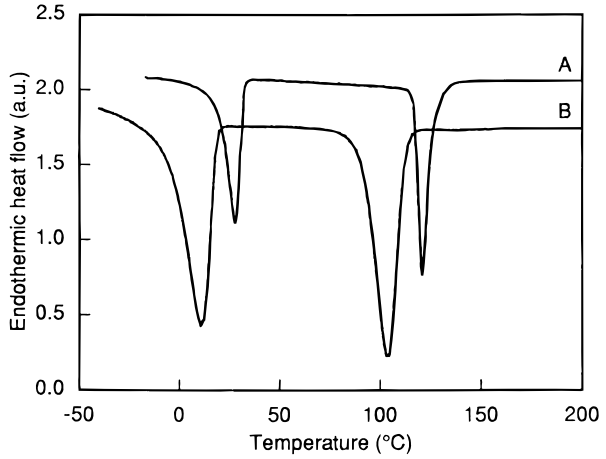

Figure 2. DSC traces recorded during cooling from the melt of a 50/50 PVF_2/PBA blend. Cooling rates of 20 °C/min (A) and 200 °C/min (B) were employed.

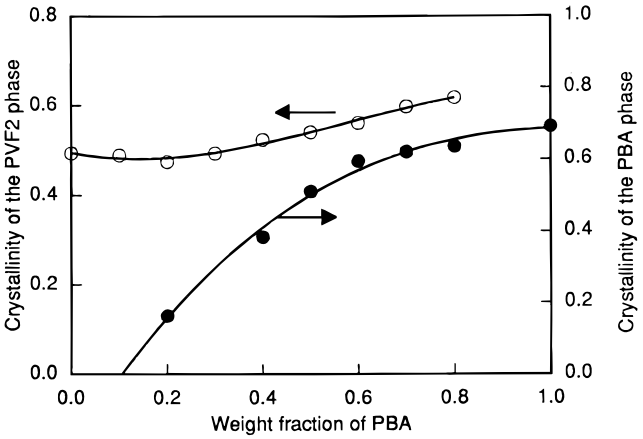

Figure 3. Normalized crystallinities of PVF_2 and PBA in their mutual blends after complete crystallization.

crystallize in different, well-separated temperature regimes.

One of the most important properties of semicrystalline/semicrystalline blends with respect to their phase behavior is the degree of crystallinity of each of the two components. Figure 3 illustrates the variation of the normalized crystallinity with blend composition for each of the blend components. The values reported here refer to samples that were allowed to crystallize for a period of time sufficiently long to ensure complete crystallization. The crystallinity of the PVF_2 component is seen to increase from ca. 50 wt % for the unblended material to ca. 60 wt % for the 20/80 blend. On the other hand, the crystallinity of the PBA component decreases markedly with increasing PVF_2 content, dropping off to zero at ca. 90 wt % PVF_2. Apparently, the addition of PBA improves the crystallization of PVF_2, which is consistent with the fact that addition of PBA lowers the T_g of the blend system.[27] The crystallization of PBA, on the other hand, appears to be severely hampered by PVF_2, which may be explained by the fact that the PVF_2 component has already completely solidified at the temperatures where PBA crystallizes (see Figure 2) and thus restricts free crystal growth for this polymer.

Glass Transition Temperature Analysis. The glass transition temperatures (T_g) of various PVF_2/PBA blends were measured by means of DSC on samples that were premelted at 200 °C and subsequently quenched into the sub-T_g region at a rate of 200 °C/min. It was observed that even under such quenching conditions,

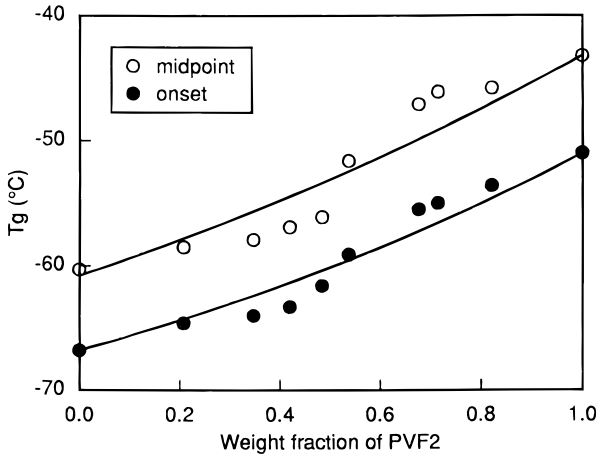

Figure 4. Variation of the glass transition temperature T_g of PVF_2/PBA blends with composition. The T_g was measured on melt-quenched samples using a heating rate of 20 °C/min.

partial crystallization cannot be completely avoided (see Figure 2). As a result of this partial crystallinity, the actual composition of the amorphous phase may differ from the overall blend composition since crystalline fractions are not available for mixing in the amorphous phase. The levels of crystallinity of the quenched samples were estimated from the areas under the melting peaks observed in the DSC scan immediately following the T_g measurement. The actual composition of the amorphous phase was estimated from the overall blend composition by taking these crystallinities into account.

The glass transition temperatures, determined from the onset as well as the midpoint of the heat capacity jump observed in the DSC traces, are plotted as a function of the amorphous phase composition in Figure 4. It is seen that, under the sample preparation conditions employed, PVF_2/PBA blends exhibit a single, composition dependent T_g intermediate between the T_g's of the respective components. The dependence of T_g on blend composition can be evaluated using the classical Gordon−Taylor (G−T) equation[28]

$$T_{g,blend} = \frac{W_1 T_{g1} + k(1 - W_1) T_{g2}}{W_1 + k(1 - W_1)} \qquad (1)$$

where W_1 is the weight fraction of component 1 (in the amorphous phase) and T_{g1} and T_{g2} are the respective T_g's of the pure components. The G−T parameter k is formally equal to $\Delta\alpha_2/\Delta\alpha_1$, where $\Delta\alpha$ is the change in the expansion coefficient at T_g, but is generally used as an empirical fitting parameter. The best fit, represented by the solid lines in Figure 4, was obtained with a value of $k = 1.3$ for both the onset- and midpoint-T_g data. A value for k close to unity is indicative of an intimately mixed amorphous phase, which, in turn, is often taken as evidence that the polymer pair is thermodynamically miscible. The notion of an intimately mixed amorphous phase in PVF_2/PBA blends is further corroborated by the fact that the width of the glass transition in these blends is comparatively small. The transition width is in the range 12−18 deg for all blends investigated here. Fried et al.[29] observed transition widths ranging from 10 to 20 deg for pure polymers and miscible blends and values in excess of 30 deg for blends approaching immiscibility.

Although the G−T equation provides a satisfactory fit of our experimental data (deviations of no more than

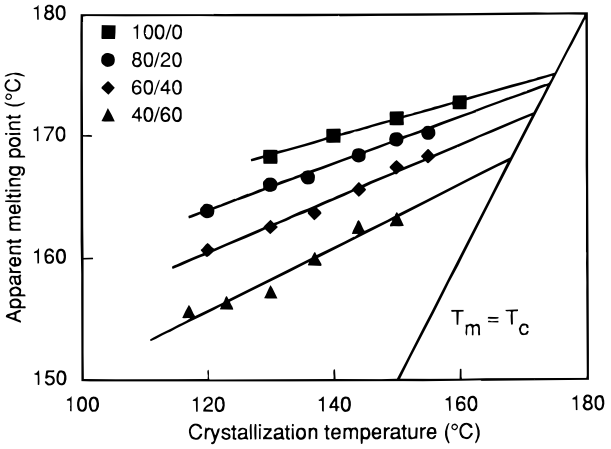

Figure 5. Hoffman−Weeks plots for PVF_2 in its blends with PBA at various compositions.

about 3 deg), the data points appear to follow a more or less sigmoidal curve rather than a smooth monotonic increase with composition, as predicted by (1). This effect may seem small, but it is reproducible and it is systematic in the sense that it is observed in both onset- and midpoint-T_g data. The deviations from the G−T equation occur in the direction of the T_g of the polymer in which the blend is richest, and the inflection point of the S-curve lies at approximately 50/50 composition. This means that the behavior of the amorphous phase is dominated by the most abundant blend component.

Melting Behavior of PVF_2. The analysis of the melting behavior of a crystalline component in semicrystalline polymer blends is an important tool in assessing polymer miscibility. In miscible blends, the melting point of the crystalline component is usually lowered with respect to the pure polymer as a result of thermodynamically favorable interactions. The extent of the melting point depression in such systems provides a measure of the interaction energy, as described by the Flory−Huggins theory[30,31] of polymer miscibility. The melting point of a polymer, however, is in general affected not only by thermodynamic factors but also by morphological parameters such as the crystal thickness. Thus, in order to separate morphological from thermodynamic effects in melting point depression analysis, one should make use of equilibrium melting point data.

The equilibrium melting point of a polymer, T_m^0, is most conveniently determined using the Hoffman−Weeks analysis.[32] This method involves isothermal crystallization of the sample at various temperatures T_c and plotting the observed melting point T_m as a function of T_c. The Hoffman−Weeks equation

$$T_m = \eta T_c + (1 - \eta)T_m^0 \qquad (2)$$

predicts a linear relation between T_m and T_c. The equilibrium melting point T_m^0 is obtained from the intersection of this line with the $T_m = T_c$ equation. The slope of the Hoffman−Weeks plot, η, assumes values between 0 and 1 and may be regarded as a measure of the stability, i.e., the lamellar thickness, of the crystals undergoing the melting process.[32] A value of $\eta = 0$ implies that the crystals are perfectly stable ($T_m = T_m^0$ for all T_c), whereas a value of $\eta = 1$ reflects inherently unstable crystals.

Figure 5 shows the Hoffman−Weeks plots for PVF_2 in the bulk as well as in its blends with PBA. The results are summarized in Table 1. The value of the equilibrium melting point of pure PVF_2 obtained here

Table 1. Results of the Hoffman−Weeks Analyses of the Melting Behavior of the PVF_2 Component in PVF_2/PBA Blends

blend (PVF_2/PBA)	equilibrium mp (°C)	slope, η
100/0	175.0	0.146
80/20	174.2	0.191
70/30	173.0	0.208
60/40	171.8	0.219
50/50	170.5	0.257
40/60	168.1	0.257
20/80	166.6	0.295

(175 °C) is in good agreement with previously reported values which are in the range from 174 to 180 °C.[4,15,20,31] It is seen that, in the blends, the equilibrium melting point of the PVF_2 phase decreases steadily with PBA content. The maximum extent of this melting point depression is 8 deg in the 20/80 blend, where the PVF_2 has $T_m^0 = 167$ °C. Another interesting feature of the melting behavior of PVF_2 in its blends with PBA is that the slope of the Hoffman−Weeks plots (η) increases with PBA content. This suggests that the PVF_2 crystals become less stable, i.e., have smaller lamellar thicknesses, when mixed with PBA. Due to this morphological effect, the depression of the actually observed melting point may be as high as 15 deg.

The melting point depression of a crystallizable polymer in a compatible mixture with a noncrystallizable polymeric diluent, according to the Flory−Huggins theory,[30,31] can be written as

$$\frac{1}{T_m^0(\text{blend})} - \frac{1}{T_m^0(\text{pure})} = -\frac{RV_2}{\Delta H^0 V_1}\left[\frac{\ln \phi_2}{m_2} + \left(\frac{1}{m_2} - \frac{1}{m_1}\right)\phi_1 + \chi_{12}\phi_1^2\right] \qquad (3)$$

where T_m^0(pure) and T_m^0(blend) are the equilibrium melting points of the crystallizable polymer in the bulk and in the blends, respectively, ΔH^0 is the heat of fusion of the crystalline component, V is the molar volume of the repeat unit, and m and ϕ are the degree of polymerization and volume fraction, respectively, of the components. Subscripts 1 and 2 refer to the noncrystalline (PBA) and crystalline (PVF_2) polymers, respectively. It should be noted that, since the melting point of PVF_2 is well above that of PBA, the latter is a noncrystalline polymer at the temperatures of interest so that this equation may be applied to the melting point data of the PVF_2 phase. Equation 3 can be rewritten as

$$-\left[\frac{\Delta H^0 V_1}{RV_2}\left(\frac{1}{T_m^0(\text{blend})} - \frac{1}{T_m^0(\text{pure})}\right) + \frac{\ln \phi_2}{m_2} + \left(\frac{1}{m_2} - \frac{1}{m_1}\right)\phi_1\right] = \chi_{12}\phi_1^2 \qquad (4)$$

This equation may be used to determine the interaction parameter χ_{12}. If the interaction parameter is independent of blend composition, a plot of the left-hand side of (4) vs ϕ_1^2 should give a straight line, passing through the origin, with a slope equal to χ_{12}. From the interaction parameter, one may also calculate the interaction energy density B, characteristic of the polymer pair, which is equal to $\chi_{12}RT/V_1$.[31]

In order to calculate the left-hand side of (4) from the experimental melting point data, the following parameter values have been used: $\Delta H^0 = 5962$ J/mol,[15] $V_1 = 164.8$ cm^3/mol,[33] $V_2 = 36.4$ cm^3/mol,[31] $m_1 = 70$, and m_2

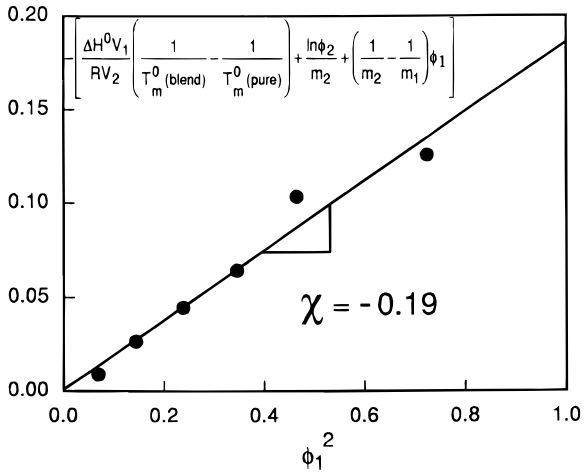

Figure 6. Melting point depression of PVF_2 as a function of blend composition, plotted according to the Flory–Huggins equation, (4). See text for explanations.

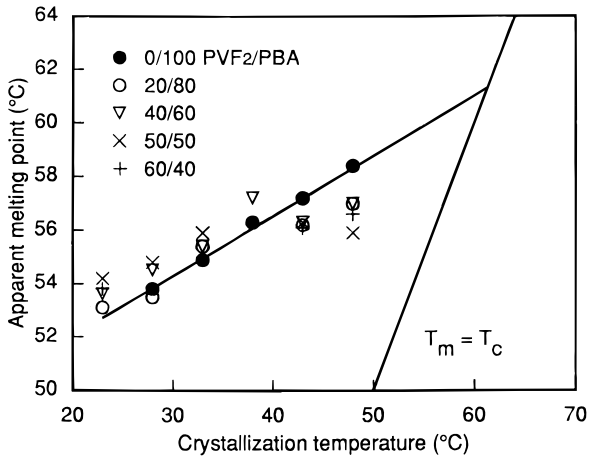

Figure 7. Hoffman–Weeks plots for PBA in its blends with PVF_2 at various compositions. The solid line represents the Hoffman–Weeks extrapolation for pure PBA (●).

= 2200. Weight fractions were converted to volume fractions using $\rho(PVF_2) = 1.80$ g/cm^3 and $\rho(PBA) = 1.23$ g/cm^3.

The plot of (4) using the experimental melting point data for PVF_2 in its mixtures with PBA is shown in Figure 6. As is seen, a straight line with a negligible intercept is obtained, in accordance with the Flory–Huggins theory. This implies that the interaction parameter is independent of the composition of the mixture for all compositions investigated (80/20 to 20/80). From the slope of Figure 6, we find

$$\chi_{12} = -0.19 \text{(at 175 °C)}$$

$$B = -4.2 \text{ J/(cm}^3 \text{ of PBA)}$$

The negative value for χ_{12} at 175 °C implies that the PVF_2/PBA polymer pair is thermodynamically miscible and that the two polymers can form a compatible mixture in the melt state, i.e., above the melting point of the high-T_m component, PVF_2.

Melting Behavior of PBA. Similar to the approach adopted for PVF_2, the melting behavior of the low-T_m PBA component has been studied by means of Hoffman–Weeks analysis at various blend compositions. This method is, however, complicated by the fact that, upon cooling the sample from the melt, the PVF_2 component may partially crystallize before the temperature region of PBA crystallization is reached. Figure 2 reveals that this is indeed the case: even under quenching conditions (cooling at 200 °C/min), substantial crystallization of the PVF_2 component takes place. Since crystallization of PVF_2 cannot be avoided when cooling to $T < T_m$(PBA), we have chosen to allow the PVF_2 to crystallize from the melt under controlled conditions in order to establish a reproducible thermal history. This was achieved by crystallization at 100 °C for 1 h. Then, the samples were further cooled to a temperature T_c suitable for PBA crystallization (20–50 °C).

The Hoffman–Weeks plots for the PBA component in various PVF_2/PBA blends obtained as such are shown in Figure 7. For pure PBA we find an equilibrium melting temperature of 61 °C. Interestingly, the Hoffman–Weeks data for pure PBA and for PBA in various blends containing up to 60 wt % PVF_2 all appear to be following more or less the same linear relation. This is especially true for the melting points obtained at crystallization temperatures in the range 20 °C < T_c < 40 °C. Extrapolation of these data to the $T_m = T_c$ line gives $T_m^0 = 61.5$ °C within a 1 deg margin for all blends. However, the melting points of the blends obtained at T_c > 40 °C are consistently lower than those of pure PBA. When these data points are included in the Hoffman–Weeks extrapolation, somewhat lower T_m^0 values are obtained for PBA in the blends (see Table 2). Thus, the Hoffman–Weeks data presented in Figure 7 are not conclusive as to whether or not PBA undergoes equilibrium melting point depression due to mixing with PVF_2.

Table 2. Results of the Hoffman–Weeks Analyses of the Melting Behavior of the PBA Component in PVF_2/PBA Blends

blend (PVF_2/PBA)	T_m^0 (°C)[a]	T_m^0 (°C)[b]
0/100	61.0	61.0
20/80	61.8	59.1
30/70	62.5	59.6
40/60	62.7	58.9
50/50	60.5	57.0
60/40		57.8

[a] From extrapolation of melting point data obtained at 20 °C < T_c < 40 °C. [b] From extrapolation of all melting point data.

It may be helpful, at this point, to estimate the magnitude of the melting point depression expected for PBA on the basis of the negative interaction parameter that was derived earlier for this blend system (see Figure 6). We have done this by inserting the appropriate parameter values into (3) and assuming that $\chi_{12} = -0.19$, the same value as derived for 175 °C (this is not necessarily correct since the χ parameter is temperature dependent). The result is given in Figure 8. The dotted line represents the situation where all PVF_2 present in the mixture contributes to the melting point depression; i.e., ϕ_1 in (3) corresponds to the overall volume fraction of PVF_2 in the blends. However, in the temperature range of PBA crystallization, PVF_2 is semicrystalline and only the amorphous fraction is available for mixing with PBA. This means that the actual volume fraction of PVF_2 in the liquid phase is much smaller. When this is taken into account, we arrive at a more conservative estimate of the extent of melting point depression for PBA (solid line in Figure 8). For example, the "semicrystalline model" predicts a melting point depression of ~4 deg for the 60/40 blend, whereas one finds ~11 deg if the PVF_2 component is considered to be fully amorphous. Although these calculations are a rough

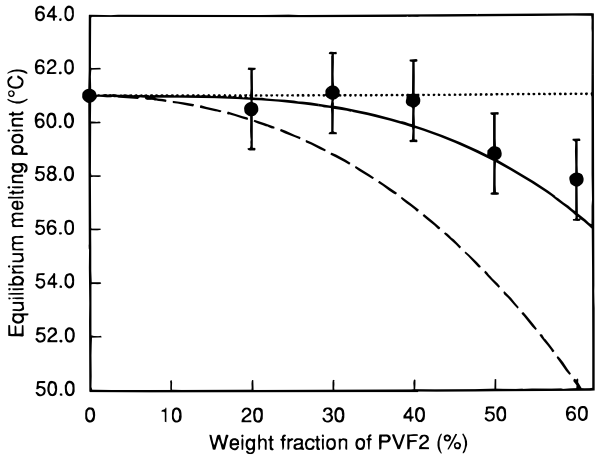

Figure 8. Equilibrium melting point of PBA in its blends with PVF_2 as a function of composition. The lines are calculated using (3) assuming that (a) all PVF_2 is available for mixing (- - -), (b) only the amorphous fraction of the PVF_2 component is available for mixing (—), and (c) there is no melting point depression (···). See text for explanation.

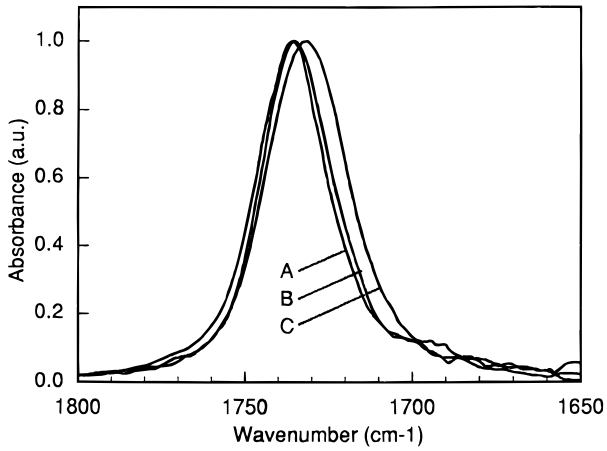

Figure 9. FT-IR spectra of PVF_2/PBA blends recorded at 180 °C for pure PBA (A), 50/50 PVF_2/PBA (B), and 80/20 PVF_2/PBA (C).

approximation, the results clearly demonstrate that the crystallinity of the high-T_m component may have a pronounced effect on the melting behavior of the low-T_m component and that the equilibrium melting point depression for the latter might be quite small.

In Figure 8, we have also plotted the actually observed equilibrium melting points for PBA, together with the error bounds as they arise from different interpretations of the Hoffman–Weeks data (Table 2). For blends containing up to 40 wt % PVF_2, the expected melting point depression is so small (<1 deg) that it is impossible to say whether our experimental data follow the predicted behavior or rather indicate that there is no melting point depression at all. However, at higher PVF_2 concentrations, the experimental data are in good agreement with the predictions of the semicrystalline model, indicating that the equilibrium melting point of the PBA phase is in fact lowered due to mixing with PVF_2. Our calculations show that the observed melting point depression is consistent with a χ parameter similar to that derived on the basis of PVF_2 melting point data ($\chi_{12} = -0.19$), if one takes into account that only a fraction of the PVF_2 component is available for mixing because it is partially crystalline.

FT-IR Measurements. The results of DSC studies presented here have indicated that blends of PVF_2 and PBA are thermodynamically miscible. In general, miscibility in polymeric blends arises from specific interactions between the two polymers. Infrared spectroscopy can be used to establish the nature and level of such molecular interactions in polymer blends.[34] We have examined the position and line shape of the carbonyl stretching band of PBA at various PVF_2/PBA blend compositions in order to detect specific interactions involving the carbonyl group. The infrared spectra were collected at room temperature as well as 180 °C. At room temperature, both blend components are semicrystalline so that molecular mixing between the two polymers is limited. At 180 °C, however, the blends form a homogeneous mixture in which many more molecular interactions are possible.

The FT-IR spectra collected at room temperature reveal only very small, if not insignificant, shifts in the carbonyl frequency upon addition of PVF_2, the maximum shift being about 1 cm^{-1}. In addition, no broadening of the absorption band was observed. The spectra recorded at 180 °C, however, show a more significant effect of blending on the position and shape of the carbonyl band, as is illustrated in Figure 9. It is seen that addition of PVF_2 results in a progressive shift of the carbonyl band toward lower frequencies, from 1736 cm^{-1} for pure PBA to 1733 cm^{-1} for the blend containing 80 wt % PVF_2. Concomitantly, the width-at-half-height of the peak increases from 25 to 29 cm^{-1}. The absorption bands are symmetrical except at 80 wt % PVF_2 where the band is slightly skewed toward lower frequencies.

The frequency shift and line broadening observed in the high-temperature spectra indicate that, in PVF_2/PBA blends, some kind of intermolecular interaction involving the PBA carbonyl group is present. The magnitude of the frequency shift ($\Delta\nu = 3$ cm^{-1}) suggests that these interactions are rather weak. In blends with strong hydrogen bonding, such as poly(caprolactone)/poly(vinylphenol)[35] or cellulose/poly(vinylpyrrolidone),[36] carbonyl shifts of about $\Delta\nu = 25$ cm^{-1} are observed. On the other hand, blends with weak hydrogen bonding, such as poly(caprolactone) with different poly(vinyl halide)s,[37,38] exhibit carbonyl frequency shifts in the range $\Delta\nu = 4-6$ cm^{-1}, which is comparable to the value observed here for PVF_2/PBA blends. It has been pointed out by Prud'homme[39] that poly(vinylidene halide)s, such as $PVCl_2$ and PVF_2, are not capable of forming hydrogen bonds, and therefore, it is more likely that the specific interaction between polyesters and poly(vinylidene halide)s is a dipole–dipole interaction between the C=O and C–Cl or C–F groups. It seems reasonable to assume that the observed molecular interactions in PVF_2/PBA blends are of this type. Since the carbonyl frequency shift is very small, this result emphasizes the weakness of the interactions, leading to thermodynamic miscibility in these blends.

Conclusions

The phase diagram of PVF_2/PBA mixtures exhibits multiple phase transitions and contains several indications of thermodynamic miscibility of this polymer pair. A single glass transition is observed across the compositional diagram. Liquid–liquid phase separation is observed above a LCST of 235 °C. Analysis of the equilibrium melting point of PVF_2 as a function of blend composition using the Flory–Huggins equation yields a negative value of $\chi_{12} = -0.19$ for the polymer–polymer interaction parameter. The low-T_m component, PBA,

also undergoes melting point depression, but to a lesser extent. The magnitude of the melting point depression of PBA, however, appears to be consistent with a similar value of the χ parameter, if it is taken into account that PVF_2 is semicrystalline in the PBA melting range and, as a consequence, interacts with PBA only to a limited extent. Infrared studies indicate that the thermodynamic miscibility of PVF_2 and PBA is driven by a weak interaction involving the carbonyl functionality of the polyester. It was shown that in these miscible blends, both polymers are capable of crystallization over a wide composition range. This results in a unique three-phase morphology in which the two distinct crystalline phases coexist with an intimately mixed amorphous phase.

Acknowledgment. This work has been supported through an operating grant from the Natural Sciences and Engineering Research Council of Canada (NSERC).

References and Notes

(1) Olabisi, O.; Robeson, L. M.; Shaw, M. T. *Polymer-polymer Miscibility*; Academic Press: New York, 1979.
(2) Utracki, L. A. *Polymer Alloys and Blends*; Hanser Publishers: Munich, 1989.
(3) Roerdink, E.; Challa, G. *Polymer* **1978**, *19*, 173.
(4) Eshuis, A.; Roerdink, E.; Challa, G. *Polymer* **1982**, *23*, 735.
(5) Avella, M.; Martucelli, E. *Polymer* **1988**, *29*, 1731.
(6) Edie, S. L.; Marand, H. *Polym. Prepr. (Am. Chem. Soc., Div. Polym. Chem.)* **1991**, *32*, 329.
(7) Jonza, J. M.; Porter, R. S. *Macromolecules* **1986**, *19*, 1946.
(8) Cheung, Y. W.; Stein, R. S. *Macromolecules* **1994**, *27*, 2512.
(9) Cheung, Y. W.; Stein, R. S.; Lin, J. S.; Wignall, G. D. *Macromolecules* **1994**, *27*, 2520.
(10) Cheung, Y. W.; Stein, R. S.; Chu, B.; Wu, G. *Macromolecules* **1994**, *27*, 3589.
(11) Song, H. H.; Stein, R. S.; Wu, D.-Q.; Ree, M.; Phillips, J. C.; LeGrand, A.; Chu, B. *Macromolecules* **1988**, *21*, 1180.
(12) Lando, J. B.; Olf, H. G.; Peterlin, A. *J. Polym. Sci., Part A* **1966**, *4*, 941.
(13) Doll, W. W.; Lando, J. B. *J. Macromol. Sci., Phys.* **1970**, *4*, 309.
(14) Prest, W. M., Jr.; Luca, D. J. *J. Appl. Phys.* **1975**, *46*, 4136.
(15) Welch, G. J.; Miller, R. L. *J. Polym. Sci., Polym. Phys. Ed.* **1976**, *14*, 1683.
(16) Miller, R. L.; Raisoni, J. *J. Polym. Sci., Polym. Phys. Ed.* **1976**, *14*, 2325.
(17) Weinhold, S.; Litt, M. H.; Lando, J. B. *J. Polym. Sci., Polym. Lett.* **1979**, *17*, 585.
(18) Lovinger, A. J.; Keith, H. D. *Macromolecules* **1979**, *12*, 919.
(19) Lovinger, A. J. *J. Polym. Sci., Polym. Phys. Ed.* **1980**, *18*, 793.
(20) Morra, B. S.; Stein, R. S. *J. Polym. Sci., Polym. Phys. Ed.* **1982**, *20*, 2243.
(21) Briber, R. M.; Khoury, F. *J. Polym. Sci., Polym. Phys. Ed.* **1993**, *31*, 1253.
(22) Braun, D.; Jacobs, M.; Hellmann, G. P. *Polymer* **1994**, *35*, 706.
(23) Wada, Y. *Electronic Properties of Polymers*; J. Wiley & Sons: New York, 1982.
(24) Paul, D. R.; Barlow, J. W.; Bernstein, R. E.; Wahrmund, D. C. *Polym. Eng. Sci.* **1978**, *18*, 1225.
(25) Yagforov, M. S. *Vysokomol. Soedin., Ser. A* **1975**, *17*, 2476.
(26) Kyu, T.; Saldanha, J. M. *J. Polym. Sci., Polym. Lett. Ed.* **1988**, *26*, 33.
(27) Oudhuis, A. A. C. M.; Thiewes, H. J.; van Hutten, P. F.; ten Brinke, G. *Polymer* **1994**, *35*, 3936.
(28) Gordon, M.; Taylor, J. S. *J. Appl. Chem.* **1952**, *2*, 493.
(29) Fried, J. R.; Karasz, F. E.; MacKnight, W. J. *Macromolecules* **1978**, *11*, 150.
(30) Flory, P. J. *Principles of Polymer Chemistry*; Cornell University Press: Ithaca, NY, 1953.
(31) Nishi, T.; Wang, T. T. *Macromolecules* **1975**, *8*, 909.
(32) Hoffman, J. D.; Weeks, J. J. *J. Res. Natl. Bur. Stand. A* **1962**, *66*, 13.
(33) Van Krevelen, D. W. *Properties of Polymers*; Elsevier: New York, 1976.
(34) Koenig, J. L. *Spectroscopy of Polymers*; American Chemical Society: Washington, DC, 1992.
(35) Moskala, E. J.; Varnell, D. F.; Coleman, M. M. *Polymer* **1985**, *26*, 228.
(36) Masson, J.-F.; Manley, R. St. J. *Macromolecules* **1991**, *24*, 6670.
(37) Coleman, M. M.; Zarian, J. *J. Polym. Sci., Polym. Phys. Ed.* **1979**, *17*, 837.
(38) Cousin, P.; Prud'homme, R. E. In *Multicomponent Polymer Materials*; Paul, D. R., Sperling, L. H., Eds.; American Chemical Society: Washington, DC, 1986.
(39) Prud'homme, R. E. *Polym. Eng. Sci.* **1982**, *22*, 90.

MA950651T